

Proceeding Paper

^{99m}Tc -Selenium-NPs as SPECT Tracers: Radio Synthesis and Biological Evaluation [†]

Akhilesh Kumar Singh ¹, Mohd. Faheem ^{1,2} , Amit Jaiswal ¹, Malleswari Ponnala ³, Sanjay Gambhir ¹ and Manish Dixit ^{1,*} 

¹ Department of Nuclear Medicine, Sanjay Gandhi Postgraduate Institute of Medical Sciences, Lucknow 226020, India

² Department of Chemistry, University of Lucknow, Lucknow 226007, India

³ Science Department, Borough of Manhattan, Community College, CUNY, New York, NY 10007, USA

* Correspondence: dixitm@sgpgi.ac.in

[†] Presented at the 27th International Electronic Conference on Synthetic Organic Chemistry (ECSOC-27), 15–30 November 2023; Available online: <https://ecsoc-27.sciforum.net/>.

Abstract: As the usage of nano-sized complexes in biomedical applications has grown significantly over the past ten years, nanoparticles are now playing a significant role in the enhancement and revolution of medical applications. It may be due primarily to the novel and exceptional electrical, optical, photo-responsive, and catalytic capabilities displayed by particles with sizes ranging from 1 to 100 nm. The radiolabelled nanoparticles refer to the process of incorporating radioactive isotopes into nanoparticles. This technique enables the nanoparticles to be tracked, imaged and monitored using various imaging techniques, such as Single-Photon Emission Computed Tomography (SPECT/CT) or Positron Emission Tomography (PET). They play a crucial role in understanding the biodistribution, pharmacokinetics, and targeted delivery of nanoparticles to biological systems. In this study, selenium-based nanoparticles (Se-NPs) were explored for imaging potential as these are usable due to their size, surface, and kinetics, as well as their ability to be functionalised. The ^{99m}Tc radionuclide was used to radiolabel the bio-inspired highly dispersed over grown endophytic fungus *Fusarium oxysporum* selenium NP using conventional radiochemistry protocol. The radiolabelling yield was found to be $94.5 \pm 3\%$ and analysed by various analytical tools. The synthesized ^{99m}Tc -Se-NPs were assessed through *In-vitro* stability, and their *In-vivo* biodistribution was performed. The accumulation of post six-hour data was primarily seen in the liver (around 3.4% ID/g) and lungs (about 2.2% ID/g). These Se-NPs can be used as an imaging agent for lung and liver disorders because these NPs quickly pass through the kidneys are expelled via urine and show a long retention time in the body. These properties of ^{99m}Tc -Se-NPs can be used for non-invasive imaging via SPECT.

Keywords: nanoparticles; radiolabelling; ^{99m}Tc ; SPECT; imaging



Citation: Singh, A.K.; Faheem, M.; Jaiswal, A.; Ponnala, M.; Gambhir, S.; Dixit, M. ^{99m}Tc -Selenium-NPs as SPECT Tracers: Radio Synthesis and Biological Evaluation. *Chem. Proc.* **2023**, *14*, 54. <https://doi.org/10.3390/ecsoc-27-16172>

Academic Editor: Julio A. Seijas

Published: 14 December 2023



Copyright: © 2023 by the authors. Licensee MDPI, Basel, Switzerland. This article is an open access article distributed under the terms and conditions of the Creative Commons Attribution (CC BY) license (<https://creativecommons.org/licenses/by/4.0/>).

1. Introduction

Nanotechnology in diagnostics via *in vivo* research shows enhancements in the treatment of diseases [1]. This technology plays a dynamic role in pharmaceuticals that have been exploited in the design of tumour-targeting agents which can be used for selective drug delivery, targeted hyperthermia treatment, or specific imaging of tumour sites, resulting in improved therapy and diagnosis [2–4]. The nano-pharmaceuticals used in the way of radiation form radio-nanoparticles (such as Se-NPs in this study) that can be used for imaging as well as therapy. To improve diagnostic outcomes and therapeutic effects in a number of diseases, the most significant of which being cancer, recent advancements in nuclear medicine have concentrated on the discovery and development of novel radiopharmaceuticals such as theranostics. A radiopharmaceutical's effectiveness is influenced by the kind of carrier it contains and the radionuclide that is chelated or labelled with the moieties. The carrier

could be an organic or inorganic molecule/nanoparticle such as selenium NPs that can accumulate on a particular diseased region to work therapeutically or diagnostically [5]. The radiopharmaceutical's theranostics properties are determined by the radionuclide's particle emission, which is bound to the carrier [6]. To achieve the desired outcome with the least amount of radiation exposure to healthy tissues, the optimum radiopharmaceutical should concentrate on the tumour area [7]. The optimum size and physical characteristics of Se-NPs make them particularly useful as radiopharmaceuticals using radionuclides for molecular imaging. These characteristics enable improved kinetics and biological activities at subcellular levels. Additionally, the incorporation of a targeting molecule, such as a peptide or an antibody specific to a tumour, onto the surface of selenium nanoparticles has significantly improved their ability to be target-specific, which was previously just a matter of perfusion due to the increased permeability and retention effect of the tumour vasculature [8]. The enormous surface area of selenium nanoparticles allows for further effective alterations, such as the attachment of imaging moieties, in addition to functionalising them with targeted ligands [9]. The synthesis of ^{99m}Tc -based nanoparticle labelling represents a significant advancement in the field of nuclear medicine and nanotechnology. These nanoparticles are modified using ^{99m}Tc , a radioisotope with ideal properties for medical imaging for diagnosis due to its ideal half-life and minimal radiation exposure [10–12]. The synthesis process involves precise control over the size, shape, and surface properties of the nanoparticles, ensuring their stability and biocompatibility [13]. Once synthesised, these ^{99m}Tc -labelled nanoparticles find versatile applications in the medical field. They are commonly used as highly efficient and targeted imaging agents for various diseases, including cancer, cardiovascular disorders, and neurodegenerative conditions [14]. Their small size allows them to navigate through the body, reaching specific cells or tissues of interest. Moreover, their radioactive properties enable precise imaging, aiding clinicians in accurate diagnosis and treatment planning. Additionally, ongoing research explores the potential of these nanoparticles in assessing the therapeutic response of targeted radiotherapy, promising a future where these innovative nanoparticles could revolutionise the landscape of personalised medicine and patient care [15–17]. The majority of selenium nanoparticles have limited blood circulation time and, enhanced toxicity and are subjected to rapid uptake by the reticuloendothelial system in vivo [18]. The synthesis of nanoparticles via chemical methods are very common, but this method has issues, e.g., the use of excess solvent and other harmful chemicals [19]. To overcome this problem, biosynthesised nanoparticles are adopted, which are highly stable, water-soluble, and capped by phytochemicals or natural protein molecules. In this article, our group successfully radiolabelled nanoparticles which are isolated from biological processes and labelled them with ^{99m}Tc radionuclide. We explored these tracers as non-invasive imaging tools for various biological disorders.

2. Material and Methods

All of the chemicals and reagents used were of analytical reagent grade and utilised without further purification. The selenium tetrachloride (SeCl_4) was used for the biosynthesis of Se-NPs, purchased from Sigma-Aldrich, Bangalore, India, Pvt. Ltd. The Technetium-99m was eluted from a $^{99}\text{Mo}/^{99m}\text{Tc}$ generator as pertechnetate (SDS Life Sciences, Pvt. Ltd., New Delhi, India). Instant thin-layer chromatography paper (iTLC) was purchased from Sigma-Aldrich (India, Pvt. Ltd.). The radiolabelling was confirmed by rTLC (Eckert and Ziegler Radiopharma, MiniScan PRO, Berlin, Germany, 61-20-0) using a PMT-based Detector B-FC-3200, and 660V was used for the determination of purity of the radiopharmaceuticals. The radioactive samples were analysed using a NaI (Tl) γ -ray scintillation counter (CAPTUS[®] 3000 gamma counter CAPINTEC, Ramsey, NJ, USA).

2.1. Biosynthesis of Se-NPs

As already documented in the literature synthesis of Se-NPs by Abasar et al. [20], in brief, about 20 grams of biomass was added to 100 mL of newly made aqueous SeCl_4 solution (2 mM) in a 500 mL Erlenmeyer flask (sterilised) for the biosynthesis of Se-NPs.

The reaction was preceded at room temperature and put on the shaker (~200 rpm). The mycelia were removed from the appropriate medium by a straightforward filtration process 72 h after the reaction had been completed. After preparation, the Se-NPs were lyophilised or dried. The synthesised Se-NPs were characterised by using different techniques like FTIR, UV-Vis spectrophotometer, TEM, and XRD.

2.2. Radiolabelling of Selenium Nanoparticles

The radiolabelling was carried out in a V-shaped vial. The radiolabelling procedure of Se-NPs with ^{99m}Tc was adopted from the reported literature [21], with slight modifications. The Se-NPs were added to a dry and clean V-shaped vial, and then, we added 100 μL (200–370 MBq) of a fresh elute ^{99m}Tc as $\text{Na}^{99m}\text{TcO}_4$ in saline solution (Figure 1). The V-shape vial was stirred at 40 $^\circ\text{C}$.

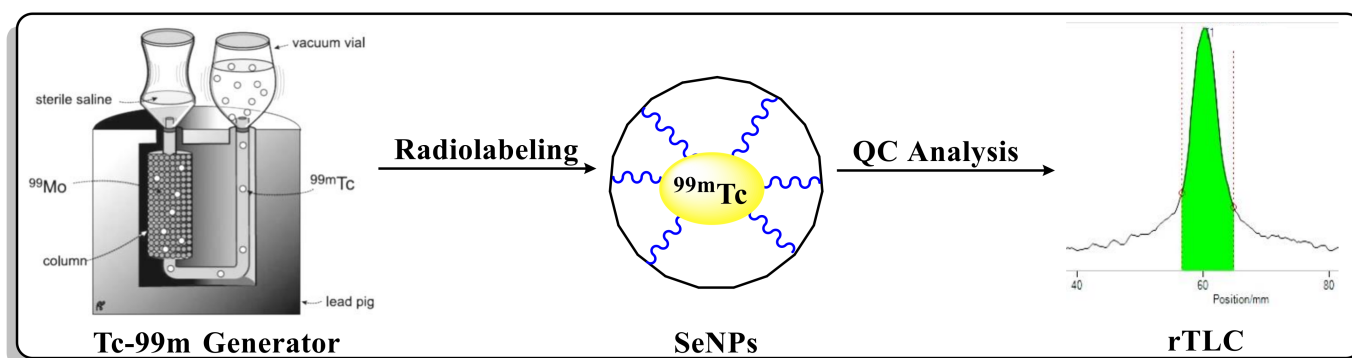


Figure 1. Systematic synthesis of radiolabelled Se-NPs with ^{99m}Tc radionuclide.

2.3. Radiochemical Yield of [^{99m}Tc]TcSe-NPs

The instant thin-layer chromatography (iTLC) paper, 12 cm long and 1 cm wide, was used for the radiochemical yield (RCY) of radiolabelled Se-NPs. The silica-based TLC plate was marked at a distance of 2 cm from the lower end and lined into sections of 1 cm each up to 10 cm. After the reaction, a drop of the reaction mixture was spotted onto the TLC stripe and developed in acetone as a developing solvent. After developing, the TLC was cut into two pieces of 1 cm each. The sections were then counted using a NaI (TI) γ -ray scintillation counter to determine the radiochemical yield (RCY). To calculate the percentage of RCY, the radioactivity of radiolabelled nanoparticles [^{99m}Tc]Tc-Se-NPs was divided by the total activity and multiplied by 100. The radiolabelling efficiency with Se-NPs was in the range of >95%, and stability was evaluated at various time scales under physiological solutions and conditions.

2.4. In Vivo Biological Studies

All animal experiments were conducted in compliance with the Committee for Control and Supervision of Experiments on Animals (CCSEA) and with the approval of the institutional ethics committee (Reference No.: SGPGIMS/AH/24th IAEC/P-20/084/2018). For *In-vitro* evaluation, a group of healthy Wistar rats were used for the evaluation of [^{99m}Tc]Tc-Se-NPs at various time intervals. The [^{99m}Tc]Tc-Se-NPs complex (75 μL approx. 11–14 MBq) solution was injected via intravenous (I.V.) into the tail vein of the rats. After imaging, the rats were sacrificed and their organs were removed, washed with saline, weighed, and measured for their radioactivity using a gamma counter. The following formula was used to calculate the proportion of the administered dose per gram of tissue (%ID/g), and the tissue uptakes were assessed.

$$\%ID/g = \frac{\text{Counts per gram of organ}}{\text{Counts dose given (total)}} \times 100$$

3. Results and Discussion

The ^{99m}Tc radionuclides have versatile chemistry, which has been exploited for the labelling of biomolecules. Technetium is the 43rd element in the periodic table and belongs to the group of transition metals owing to its electronic configuration of $[\text{Kr}]4d^55s^2$. Technetium provides several opportunities for complex formation with a large number of different ligands due to its oxidation state (OS) varying from +one up to +seven. The structure of technetium complexes can also be characterised by the coordination number (N), which can vary from four to seven. The typical approach employed in the synthesis of first-generation radiopharmaceuticals in the past was direct labelling through the reduction of pertechnetate with stannous chloride in an acidic environment. The labelling of Se-NPs was optimised under reduction using 0.1 mg of $\text{SnCl}_2 \cdot \text{H}_2\text{O}$ as a reducing agent, as documented in the literature, with slight modifications. The various concentrations of nanoparticles were explored for radiolabelling, and the best yield was obtained when the concentration of the NPs was in the range of 35–40 μg .

The stability of the radiolabelled nanoparticles is shown in Figure 2a,b respectively, while the chelation stability was maintained in physiological saline and human serum albumin solutions. The stability was evaluated by using the iTLC method at various time points, as shown in Figure 2. The data show that the stability retains till 350 min in saline but only till 1140 min in albumin. The resulting outcome shows that the Se-NPs were superbly chelated with the metallic radionuclide (^{99m}Tc) in a physiological pH range or in an environment containing human serum albumin.

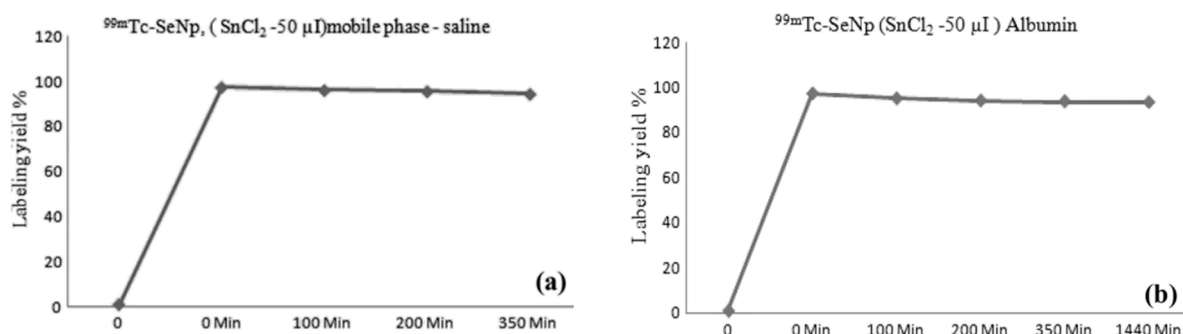


Figure 2. Stability study of ^{99m}Tc TcSe-NPs at different time intervals (a) in saline and (b) in albumin at 37 °C.

For biodistribution studies, the ^{99m}Tc TcSe-NPs complex was injected through the tail vein (11–14 MBq), and the mice were imaged at respective time scales and sacrificed to calculate the biodistribution radioactivity in different organs of interest.

The maximum percentage of injected dose per gram of organ (% ID/g) of ^{99m}Tc TcSe-NPs complex in the liver was $19.47 \pm 4\%$ at 10 min post injection (p.i.), with no significant accumulation in the spleen, but the accumulation also showed in the lungs and stomach in the range of $6 \pm 1\%$ and 9.4 ± 2 at 10 min p.i., which indicates that the radiolabelled nanoparticle was well distributed (Figure 3).

According to the data, these radiolabelled nanoparticles are much larger than the hydrodynamic diameters (HDs) of the renal clearance threshold, which is <6 to 8 nm. The kidney's activity at around 3.8 ± 2 at 6 hours post injection revealed that the nanoparticles were being excreted through the urinary system. The investigation at post 6 h revealed mostly accumulation in the liver and lungs (at 3.4% ID/g and 2.2% ID/g, respectively), which is suggestive of the nanoparticles' particle size. These nanoparticles could help with liver or lung disease (Figure 4). The Se-NPs have the benefit of having rapid blood circulation and enabling passive targeting via an enhanced permeability and retention (EPR) effect. In addition, the nanoparticles can actively target the liver and lungs through molecular interaction or affinity, which will be helpful in evaluating the functionality of these organs.

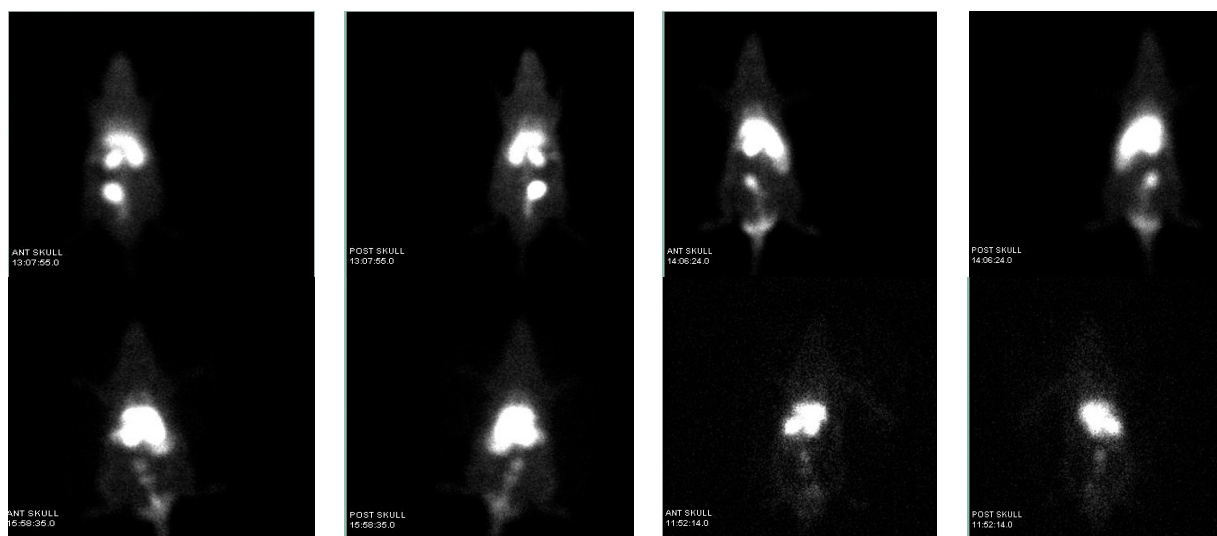


Figure 3. SPECT-based imaging of $[^{99m}\text{Tc}]\text{TcSe-NPs}$ in Wister rats.

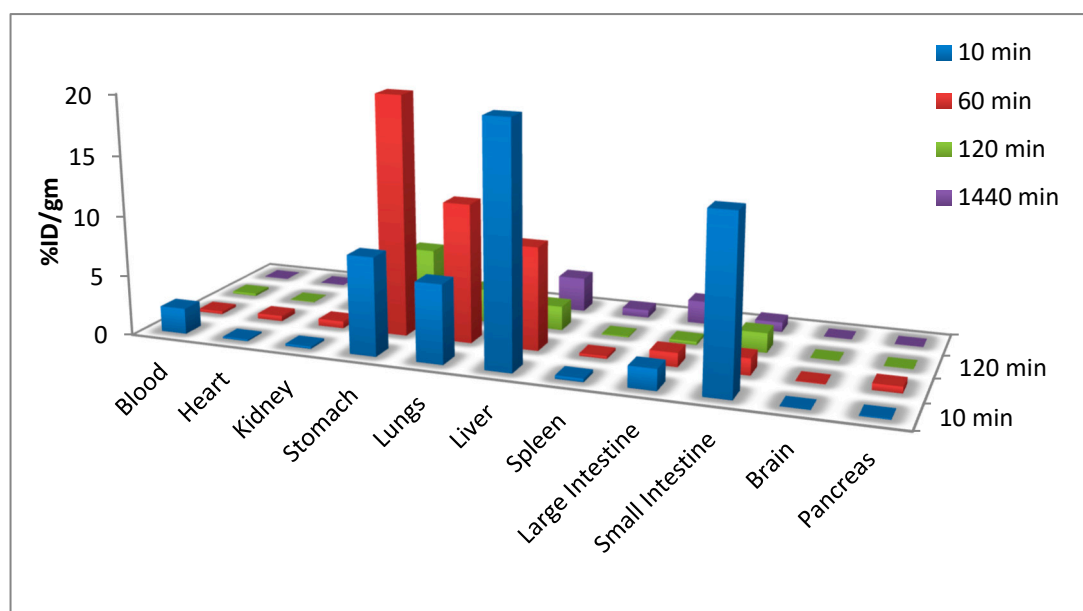


Figure 4. Biodistribution of $[^{99m}\text{Tc}]\text{TcSe-NPs}$ in Wister rat organs.

4. Conclusions

In conclusion, in this work, the size, surface, kinetics, and capacity for functionalisation of selenium-based nanoparticles (Se-NPs) were examined for their imaging ability as radiotracers. A conventional radiochemistry approach was utilised to radiolabel the naturally isolated Se-NPs with the ^{99m}Tc radionuclide with radiolabelling yield of $94.5 \pm 3\%$ and purity was examined using several analytical techniques. The stability of the synthesised $[^{99m}\text{Tc}]\text{TcSe-NPs}$ was assessed in vitro, and their biodistribution was carried out in vivo in Wistar rats at several time points. The experiment conducted at post 6 hours revealed an accumulation that was concentrated mostly in the liver (about $3.4\% \text{ ID/g}$) and lungs (around $2.2\% \text{ ID/g}$), which is suggestive of the nanoparticles' particle size. This characteristic of these $[^{99m}\text{Tc}]\text{TcSe-NPs}$ makes them useful for SPECT imaging as non-invasive biomarkers. Further exploration of these kinds of nanoparticles is underway to enhance their kinetics and clearance profile.

Author Contributions: A.K.S.: Investigation, methodology, radiolabeling, quality control/assurance. M.F.: Data correction, original draft, editing, communication. A.J.: Biodistribution. M.P.: Editing and data correction. S.G.: Radioisotope production resources. M.D.: Supervision, review and editing. All authors have read and agreed to the published version of the manuscript.

Funding: This research received no external funding.

Institutional Review Board Statement: Institutional Animal Ethics Committee (Reference No.: SGPGIMS/AH/24th IAEC/P-20/084/2018).

Informed Consent Statement: Not applicable.

Data Availability Statement: Data are contained within the article.

Acknowledgments: We are sincerely thankful to Aabsar Ahamd, Interdisciplinary Nanotechnology Centre (INC), AMU, Aligarh, for providing the Se-NPs. We also give thanks to Atul K. Baranwal for their assistance with animal experiments.

Conflicts of Interest: The authors declare no conflict of interest.

References

1. Chen, Y.; Chen, H.; Shi, J. In vivo bio-safety evaluations and diagnostic/therapeutic applications of chemically designed mesoporous silica nanoparticles. *Adv. Mater.* **2013**, *25*, 3144–3176. [[CrossRef](#)] [[PubMed](#)]
2. Wu, M.; Huang, S. Magnetic nanoparticles in cancer diagnosis, drug delivery and treatment. *Mol. Clin. Oncol.* **2017**, *7*, 738–746. [[CrossRef](#)] [[PubMed](#)]
3. Babu, A.; Templeton, A.K.; Munshi, A.; Ramesh, R. Nanoparticle-based drug delivery for therapy of lung cancer: Progress and challenges. *J. Nanomater.* **2013**, *2013*, 14. [[CrossRef](#)]
4. Van Vlerken, L.E.; Amiji, M.M. Multi-functional polymeric nanoparticles for tumour-targeted drug delivery. *Expert Opin. Drug Deliv.* **2006**, *3*, 205–216. [[CrossRef](#)] [[PubMed](#)]
5. Weingart, J.; Vabbilisetty, P.; Sun, X.L. Membrane mimetic surface functionalization of nanoparticles: Methods and applications. *Adv. Colloid Interface Sci.* **2013**, *197*, 68–84. [[CrossRef](#)] [[PubMed](#)]
6. Liu, S. Bifunctional coupling agents for radiolabeling of biomolecules and target-specific delivery of metallic radionuclides. *Adv. Drug Deliv. Rev.* **2008**, *60*, 1347–1370. [[CrossRef](#)] [[PubMed](#)]
7. Sgouros, G.; Bodei, L.; McDevitt, M.R.; Nedrow, J.R. Radiopharmaceutical therapy in cancer: Clinical advances and challenges. *Nat. Rev. Drug Discov.* **2020**, *19*, 589–608. [[CrossRef](#)] [[PubMed](#)]
8. Sun, T.; Zhang, Y.S.; Pang, B.; Hyun, D.C.; Yang, M.; Xia, Y. Engineered nanoparticles for drug delivery in cancer therapy. *Angew. Chem. Int. Ed.* **2014**, *53*, 12320–12364. [[CrossRef](#)]
9. Veisoh, O.; Gunn, J.W.; Zhang, M. Design and fabrication of magnetic nanoparticles for targeted drug delivery and imaging. *Adv. Drug Deliv. Rev.* **2010**, *62*, 284–304. [[CrossRef](#)]
10. Roy, I.; Krishnan, S.; Kabashin, A.V.; Zvestovskaya, I.N.; Prasad, P.N. Transforming nuclear medicine with nanoradiopharmaceuticals. *ACS Nano* **2022**, *16*, 5036–5061. [[CrossRef](#)]
11. Maccora, D.; Dini, V.; Battocchio, C.; Fratoddi, I.; Carloni, A.; Rotili, D.; Castagnola, M.; Faccini, R.; Bruno, I.; Scotognella, T.; et al. Gold nanoparticles and nanorods in nuclear medicine: A mini-review. *Appl. Sci.* **2019**, *9*, 3232. [[CrossRef](#)]
12. Pijera, M.S.O.; Viltres, H.; Kozempel, J.; Sakmár, M.; Vlk, M.; İlem-Özdemir, D.; Ekinci, M.; Srinivasan, S.; Rajabzadeh, A.R.; Ricci-Junior, E.; et al. Radiolabeled nanomaterials for biomedical applications: Radiopharmacy in the era of nanotechnology. *EJNMMI Radiopharm. Chem.* **2022**, *7*, 8. [[CrossRef](#)]
13. Bharti, C.; Nagaich, U.; Pal, A.K.; Gulati, N. Mesoporous silica nanoparticles in target drug delivery system: A review. *Int. J. Pharm. Investig.* **2015**, *5*, 124. [[CrossRef](#)] [[PubMed](#)]
14. Varani, M.; Campagna, G.; Bentivoglio, V.; Serafinelli, M.; Martini, M.L.; Galli, F.; Signore, A. Synthesis and biodistribution of ^{99m}Tc-labeled PLGA nanoparticles by microfluidic technique. *Pharmaceutics* **2021**, *13*, 1769. [[CrossRef](#)] [[PubMed](#)]
15. Eldin, S.S.E.; Rashed, H.M.; Hassan, A.H.; Salem, H.F.; Sakr, T.M. Multifunctional ^{99m}Tc-5-azacitidine Gold Nanoparticles: Formulation, In Vitro Cytotoxicity, Radiosynthesis, and In Vivo Pharmacokinetic Study. *Curr. Drug Deliv.* **2023**, *20*, 387–399. [[PubMed](#)]
16. Türker, S.; Özer, A.Y. Radiopharmacology and pharmacokinetic evaluation of some radiopharmaceuticals. *FABAD J. Pharm. Sci.* **2005**, *30*, 204.
17. Nokkaew, N.; Sliiratori, S.; Gonlachanvit, S.; Chaiwatanarat, T.; Nasing, T.; Chaiseri, S.; Sirisansaneeyakul, S.; Kaniugsukkasem, V. Evaluation of the First Radiolabeled ^{99m}Tc-Jerusalem Artichoke-Containing Snack Bar on Gastric Emptying and Satiety in Healthy Female Volunteers. *J. Med. Assoc. Thail.* **2018**, *101*, 1–15.
18. Feng, Q.; Liu, Y.; Huang, J.; Chen, K.; Huang, J.; Xiao, K. Uptake, distribution, clearance, and toxicity of iron oxide nanoparticles with different sizes and coatings. *Sci. Rep.* **2018**, *8*, 2082. [[CrossRef](#)]
19. Duan, H.; Wang, D.; Li, Y. Green chemistry for nanoparticle synthesis. *Chem. Soc. Rev.* **2015**, *44*, 5778–5792. [[CrossRef](#)]

20. Mansouri-Tehrani, H.A.; Keyhanfar, M.; Behbahani, M.; Dini, G. Synthesis and characterization of algae-coated selenium nanoparticles as a novel antibacterial agent against *Vibrio harveyi*, a *Penaeus vannamei* pathogen. *Aquaculture* **2021**, *534*, 736260. [[CrossRef](#)]
21. Snehalatha, M.; Venugopal, K.; Saha, R.N.; Babbar, A.K.; Sharma, R.K. Etoposide loaded PLGA and PCL nanoparticles II: Biodistribution and pharmacokinetics after radiolabeling with Tc-99m. *Drug Deliv.* **2008**, *15*, 277–287. [[CrossRef](#)] [[PubMed](#)]

Disclaimer/Publisher's Note: The statements, opinions and data contained in all publications are solely those of the individual author(s) and contributor(s) and not of MDPI and/or the editor(s). MDPI and/or the editor(s) disclaim responsibility for any injury to people or property resulting from any ideas, methods, instructions or products referred to in the content.